



Tarbur Maastrichtian to Taleh Zang Paleocene carbonate platforms: age-determination, facies analysis and depositional architecture

Sadegh Zahiri ¹, Davood Jahani ^{1,*}, Ali Rahmani ²

¹ Department of Geology, North Branch, Islamic Azad University, Tehran, Iran

² National Iranian Oil Company (NIOC), Tehran, Iran

Received: 17 January 2023, Revised: 03 July 2023, Accepted: 26 August 2023

© University of Tehran

Abstract

Maastrichtian to Thanetian carbonate platforms comprise the outcrops of scarcity, especially in Tethys, Zagros Foreland Basin of which is hardly documented. A carbonate platform-to-basin transect in Zagros Basin was done, consisting of two important outcrops, and large cliffs with a vast landscape and good photographic capacity. Based on large benthic foraminifera (LBF) and planktonic foraminifera, these carbonate platforms are referred to as Tarbur and Taleh Zang formations, which are dated to the Maastrichtian and Paleocene (Thanetian-Selandian). Multiple stratigraphic approaches, along with the facies analysis, were used to build the carbonate platform architecture and figure out the most conspicuous factors controlling the evolution of these platforms through time. Ten sedimentary facies belts were identified, ranging from the basin to the proximal and distal shallow-water contexts with carbonate ramps. The distribution of grain-associations in the spatial and temporal scale, facies belts, apparent stratal geometry, and biological evolution accompanied by age dating led to identifying two distinct carbonate models: Maastrichtian distally steepened ramp and Paleocene carbonate ramp, belonging to Tarbur and Taleh Zang carbonate formations, respectively. Due to the first dominating community of Cenozoic Zooxanthellate corals associated with red coralline algae as separate patches, the Paleocene Taleh Zang carbonate ramp was divided into two carbonate modes: Danian-lower Selandian and upper Selandian.

Keywords: Carbonate platform, Maastrichtian-Paleocene, Zagros foreland basin, Tarbur Formation, Taleh zang Formation.

Introduction

Carbonate sediments are heavily affected by complex interactions between internal and external factors, which have caused the formation of different types of carbonate platforms over geological time (Pomar, 2020; Pomar et al., 2012; Pomar and Haq, 2016; Pomar & Kendall, 2008). Because of further analogy to modern carbonate models that are affected by exponential climate changes and other ambient conditions, Cenozoic carbonate platforms have recently been fascinated by many authors. This study focuses on the transition of Maastrichtian-to-Paleocene carbonate platforms, a critical time that recorded a mass extinction event and depositional hiatus (K/Pg. boundary); however, this is poorly understood because of the lack of well-preserved outcrops around the world (Baceta et al., 2005; Pomar et al., 2017). At this boundary, the maximum richness of Cretaceous benthic and planktonic foraminifera as well as all rudist bivalves has become extinct worldwide (Pomar et al., 2017). Conversely, by the

* Corresponding author e-mail: jahani374d@gmail.com

Paleocene, a new generation of large benthic foraminifera (LBFs) and corals have recovered (Pomar et al., 2017; Baceta et al. 2005) reported the coralgal reef bioconstruction in the western Pyrenean basin, northern Spain where was reconstructed in the context of a ramp leading to a flat-topped platform by (Pomar et al., 2017). In addition, (Pomar et al., 2017) introduced these Paleocene coral communities as the first Cenozoic mesophotic buildups thrived in the west-central Tethys before the late Tortonian. Other detailed studies of Paleocene carbonate platforms are concerned with the Paleocene-Eocene Thermal Maximum (PETM) and Circum-Thethyan carbonate platform stages, which were mostly described by (Scheibner et al., 2003, 2007); (Scheibner & Speijer 2008a, 2008b, 2009). Based on variable carbonate producing organism in respond to paleo-climatic change, they have categorized this time interval to three distinct carbonate platform stages, including Platform stage I (Selandian: 58.9–56.2 Ma; SBZ 1–3), Platform stage II (Thanetian: 56.2–55.5 Ma; SBZ 4), and Platform stage III (Ypresian: 55.5–?; SBZ 5/6–?).

After connecting Arabian and Iranian microplates in the Zagros Foreland Basin (Glennie, 2000; Homke et al., 2009b); (Saura et al. 2011) and the Tarbur and Taleh Zang carbonate platforms were established through the Maastrichtian to the Paleocene, respectively. The Tarbur carbonate Formation is assigned to rudist-rich limestone, whereas the Taleh Zang Formation is composed of massive limestone cliffs rich in LBFs. Further studies have evaluated microfacies analysis, sequence stratigraphy and depositional environment of these two carbonate platforms on a local scale, as well as syn-sedimentary tectonic activities mostly on a regional scale (Bagherpour & Vaziri, 2012; Homke et al., 2009b; Saura et al., 2011; Amiri-Bakhtiyar et al., 2006; Vaziri-Moghaddam et al., 2005; Nikfard, M. 2023). Despite these valuable studies in the Zagros Basin, the depositional geometry and evolution of the Maastrichtian-Paleocene carbonate transition have received less attention. The main objectives of this research are 1) to determine the relative age of these carbonate rock successions, 2) to evaluate major carbonate-producing organisms and biotic carbonate factories, 3) to investigate depositional geometries and lateral facies heterogeneities, and 4) to reconstruct the evolution of these carbonate platforms over time. Consequently, the major carbonate organisms (type, abundance, and diversity) of the Paleocene Taleh Zang ecosystem were compared with the distribution of biotic assemblages of other Circum-Thethyan carbonate platforms organized by (Scheibner & Speijer, 2008a, 2008b).

Geological Setting and Stratigraphic Architecture:

The Zagros mountain range is a fold-thrust belt, elongated from SE Turkey to Oman and situated in SW Iran, and can be divided into five NW–SE-trending tectonic domains: the Urumieh–Dokhtar volcanic arc, metamorphic Sanandaj Sirjan Zone, Imbricated Zone (High Zagros), Simply Folded Belt, and Mesopotamian–Persian Gulf foreland basin (Berberian & King, 1981; Golonka, 2004; Homke et al., 2009a; Sherkati et al., 2006; Stöcklin, 1968). The Zagros Basin has numerous structural provinces, including Izeh, Fars, Lurestan, Dezful Embayment, and High Zagros, with regard to tectonic structures and the curving trace of basement faults, particularly the Mountain Front Fault (MFF) (Motiei, 1994, 1995; Sherkati et al., 2006). (Fig. 1). Thus, the study area is located northwest of the Izeh zone, near the High Zagros and Lurestan geological subzones, separated by the High Zagros and Balarud basement faults (Figs. 1 and 2).

As mentioned above, the Zagros orogenic belt was formed by the Arabian-Iranian convergent collision that occurred as a consequence of tectonic emplacement of ophiolitic and radiolaritic slices over the NE Arabian passive margin at the end of the Cretaceous (Berberian & King, 1981; Homke et al., 2009b; Stöcklin, 1968; Stoneley, 1990), although the precise time is debated. Southwestward, in front of these obducted/thrust sheets, the Arabian plate flexed down

in the context of an early foreland basin (Amiran basin in the Lurestan province) during the Late Cretaceous–Early Eocene, which was subsequently filled with the shallowing-upwards Amiran-Kashkan detrital succession (Alavi, 2004; Homke et al., 2009b; Saura et al., 2011), directly sourced from the oceanic uplifted region along the margin of the NW segment of the Arabian plate (Homke et al., 2009b; Saura et al., 2011).

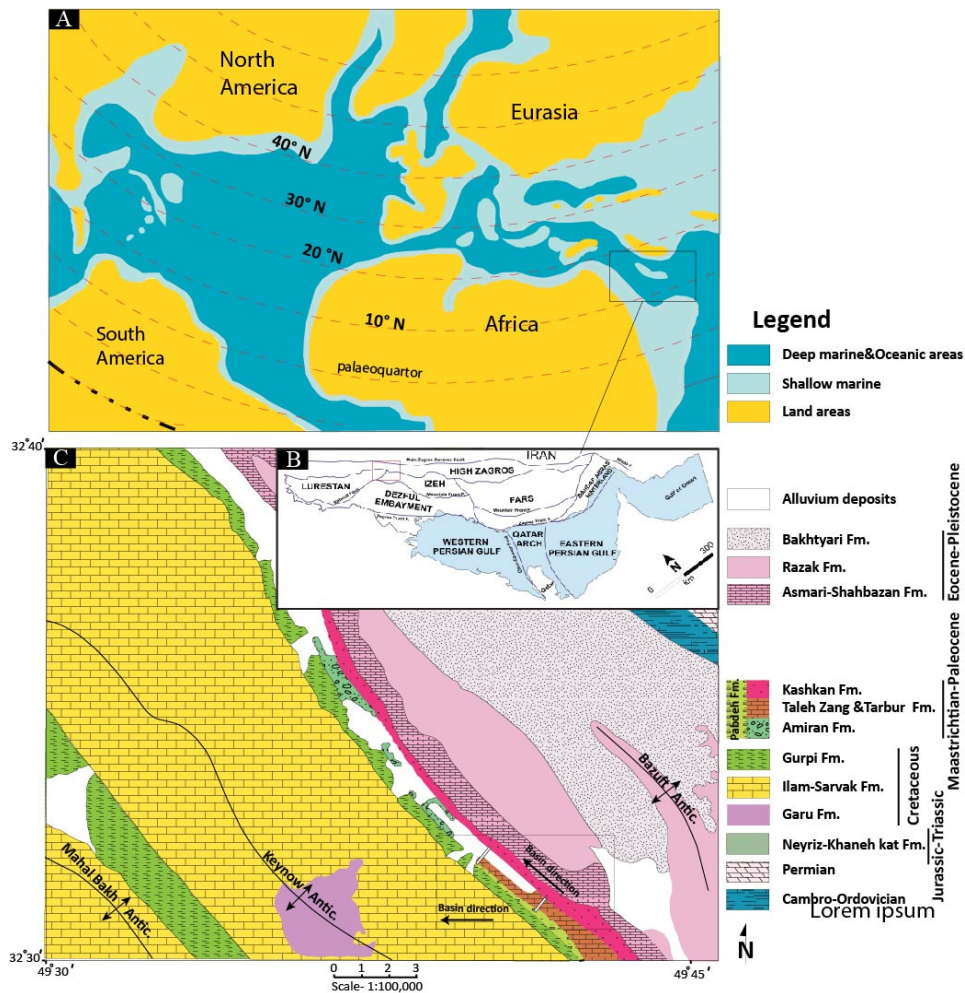


Figure 1. A: a general Paleocene paleogeographic map of Tethys and location of the study area. B: Structural province map of the Zagros Foreland Basin. The red box remarks the location of the studied area. C: Geological map of the study area (Keynow anticline). Dip direction and measured logs are shown on the map

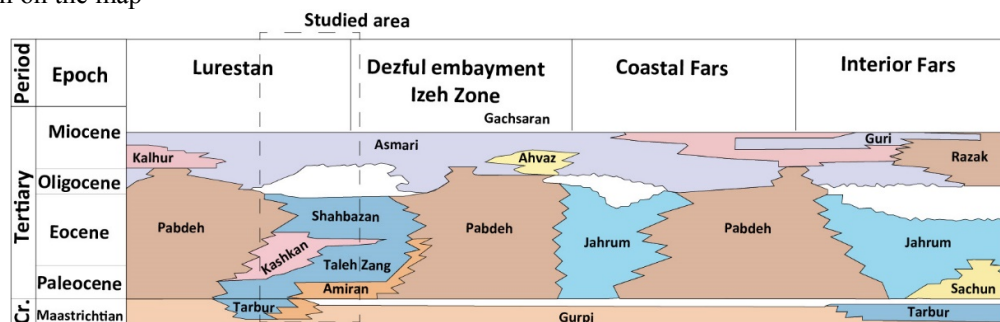


Figure 2. Chronostratigraphic column of the Zagros Foreland Basin during the Maastrichtian-Miocene. Black rectangular is the place of the studied area. Note that Tarbur, Taleh Zang and their time-equivalent formations during Maastrichtian-Paleocene

The present study comprises two distinct logged sections, namely the Taraz (Log.1), and Pich-e-Taraz (Log.2), cropped out over a distance of ca. 5km along the Keynow anticline (Figs. 1c, 3, 4). These stratigraphic sections show a mixture of carbonate and siliciclastic succession, regarding the Tarbur, Taleh Zang, Amiran, and Kashkan formations (Fig. 1c, and 3). The initiation of early foreland basin fill dates to the Maastrichtian-Paleocene, in which the Tarbur and Taleh Zang formations are the only carbonate platforms that developed northeastwards, close to the Imbricated zone. These two carbonate platforms, being limited and discontinuous in space, are mostly sandwiched between the Amiran and Kashkan detrital formations at the base and top (Figs. 2 and 3). The Maastrichtian-early Eocene Amiran Formation's sandy shale, which indicates a turbidity system, is interbedded with deep-water shales, thin-bedded sandstone, and siltstone. The proximal Tarbur and Taleh Zang carbonate formations as well as the distal Gurpi and Pabdeh formations are time-equivalent to this deep-water siliciclastic system (Fig. 2). Clastic materials are mainly sourced from the radiolarite–ophiolite complexes of the Imbricated Zone (James & Wynd, 1965) and are transported southwestward into the Amiran Basin. Therefore, in the NE, the Gurpi and Pabdeh formations with basinal deep-water shales/marls and marly limestone deposits are renamed Amiran turbidities as a consequence of being contaminated by this detrital deposit influx (Fig. 2). The Kashkan Formation, which is the continental equivalent of the Amiran Formation, consists of reddish siliciclastic deposits comprising cross-bedded laminated sandstone, conglomerate, and reddish clay, indicating a continental-alluvial system (Fig. 2). The Maastrichtian Tarbur Carbonate Formation is mostly composed of medium-bedded to large limestone rich in rudist detritus and LBF (James & Wynd, 1965; Wynd, 1965). This carbonate platform runs along the northern edge of the Zagros Basin, adjacent to the imbricated zone, and passes south into the deeper-water equivalent deposits of the Amiran/Gurpi Formation (Figs. 2). Analogous to the Tarbur Formation, the Taleh Zang Formation is attributed to medium-to-thick-scale limestone beds rich in LBF that accumulated as a carbonate platform during the Paleocene-Eocene (James & Wynd, 1965; Saura et al., 2011; Wynd, 1965). It records the first flourishing of the Cenozoic LBF shortly after the K/Pg. boundary (Figs. 4 and 5).

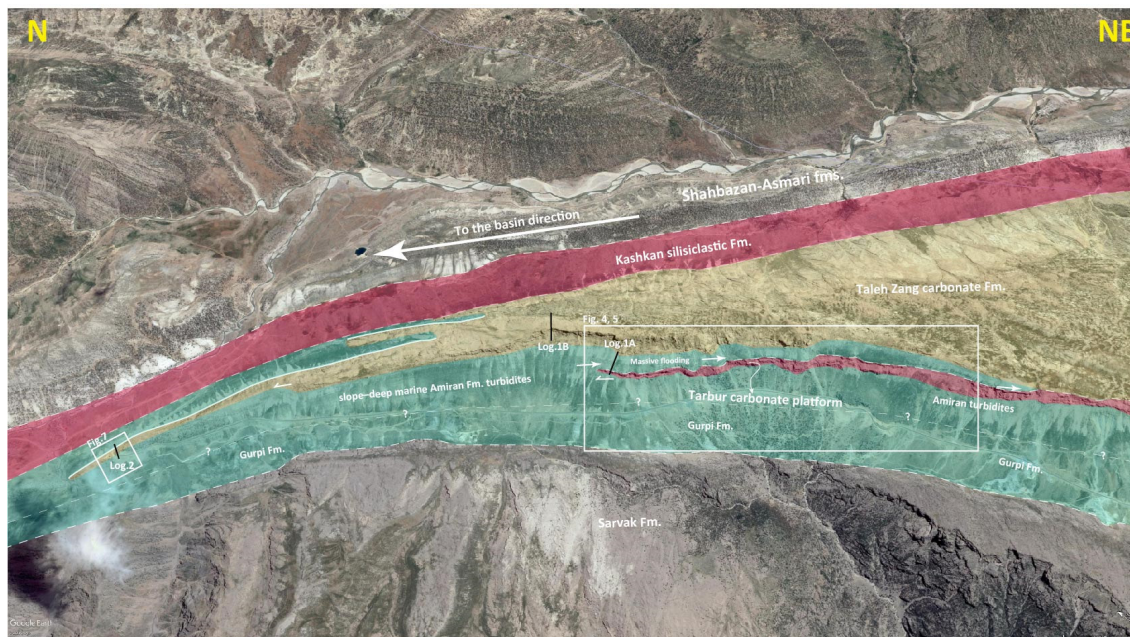


Figure 3. Satellite image of the northern flank of the Keynow anticline. Stratigraphic boundaries, bounding surfaces and two measured logs (Log. 1A & Log. 1B) are illustrated and colored



Figure 4. Photomosaic of the northern flank of the Keynow anticline; representing the exact location of measured-stratigraphic sections and line-drawing photos



Figure 5. A) General dip-view and B) its interpreted photographs of the Tarbur and Taleh Zang carbonate platforms in the location of the Taraz section (Log. 1)

This carbonate formation changes basinward (south-southeast) into its deep-water equivalent formation, that is, the Amiran Formation (Fig. 3), whereas in the opposite direction of the basin—that is, northeastward, it replaces continental deposits of the Kashkan detrital Formation (James & Wynd, 1965; Saura et al., 2011) (Fig. 2). Therefore, in the stratigraphic rock succession, the Taleh Zang Formation covers the Amiran Formation, whereas it is overlaid by the Kashkan Formation (James & Wynd, 1965) (Fig. 2).

Taraz section (Log.1 A, and B)

The stratigraphic measured log of the Taraz section has a thickness of 454m, including Tarbur, Amiran/Pabdeh, and Taleh Zang formations (Figs. 3, 4, 6). The lower part of the section (ca. 90m thick) is characterized by thick-bedded limestone succession of the Tarbur Formation, which was mostly composed of rudist debris and LBF-e.g., *Omphalocyclus* (Fig. 6, Fig.10 C, and 10 D). The Tarbur Formation was subsequently covered by a considerable interval (approx. 100 mt) of pelagic-rich shales and platy argillaceous limestone related to the Amiran/Pabdeh Formation (Figs. 3, 4, 5, and 6). As a result, the top portion accumulations of the Taraz section (ca. 260 m thick) corresponding to the Taleh Zang Formation consist of a major succession of medium- to thick-bedded limestone rich in benthic foraminifera, marly limestone to slightly shale, and thick-bedded dolo-limestone (Figs. 5 and 6). The topmost carbonate succession of the Taleh Zang Formation (about 40m thick) is frequently characterized by scattered-coral fragments (Fig. 6).

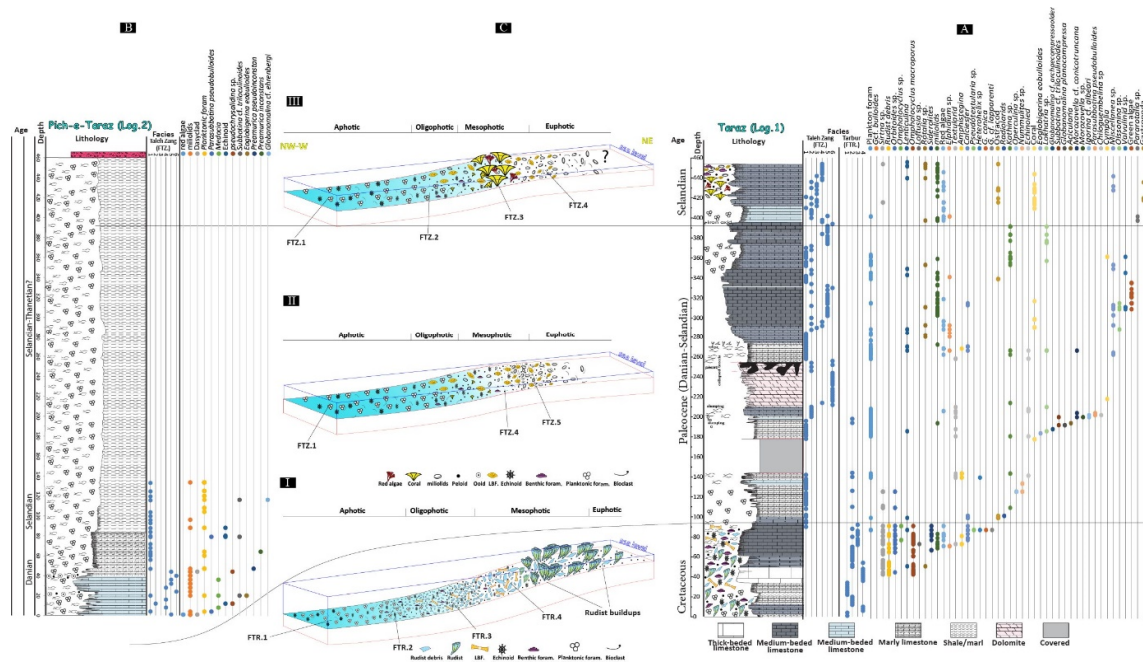


Figure 6. synthetic sedimentological logs (lithology, biological components, and facies) relative to A) Log 1 (Taraz section) and B) Log. 2 (Pich-e-Taraz) and C) conceptual models for Maastrichtian (I), Danian-Selandian (II), and Selandian (III) carbonate ramps

Pich-e-Taraz (Log. 2):

In contrast to the Traraz section, this outcrop contains only the Amiran/Pabdeh Formation with a considerable thickness of ca. 460 m, representing an alternation of deep-water shale and argillaceous limestone rich in planktonic foraminifera (Figs. 6 and 7). In fact, the carbonate succession of the Taleh Zang Formation pinched out into slope-to-deep-water deposits involving the Amiran and Pabdeh Formations just before expanding in the Pich-e-Taraz area. Finally, the upper boundary of these plankton-rich successions is capped by siliciclastic deposits of the Kashkan Formation, consisting of red-colored marls (Figs. 3 and 6).

Material and methods

This study contains two NE-NW-oriented outcrop sections (Taraz and Pich-e-Taraz), cropped out at a distance of five kilometers along the Keynow anticline (Figs. 3 and 4), near Masjed-E-Soleyman City. A total thickness of 454 m for the Taraz section (Log.1A, B) was measured, whereas a thickness of 460 m was logged for the Piche-e-Taraz section (Log.2) (Fig. 6). During stratigraphic logging, the entire skeleton and non-skeletal components, as well as visually observed depositional factors, were recorded in the stratigraphic logs (Fig. 6). Samples were collected every two meters for thin-section analysis. A total of 244 thin sections were produced for microfacies investigation and dating (213 thin sections linked to Log.1 and the rest to Log.2). Both planktonic and benthic foraminifera, in particular LBF, were used for the biostratigraphy and age determination of the logged stratal packages. The apparent geometry was interpreted using photo-panel and satellite images (Figs. 3, 4, 5, 8). Consequently, the integration of biostratigraphy, petrographic analysis, and field observations of bedding geometry and strata bounding surfaces provided an opportunity to explain facies heterogeneities and depositional model architecture as well as to reconstruct carbonate platform evolution over time.



Figure 7. Satellite image (A) and outcrop photograph (B) of the stratigraphical log. 2 (Pich-e-Taraz). It shows an alternation of argillaceous limestone and deep-water shale/marls

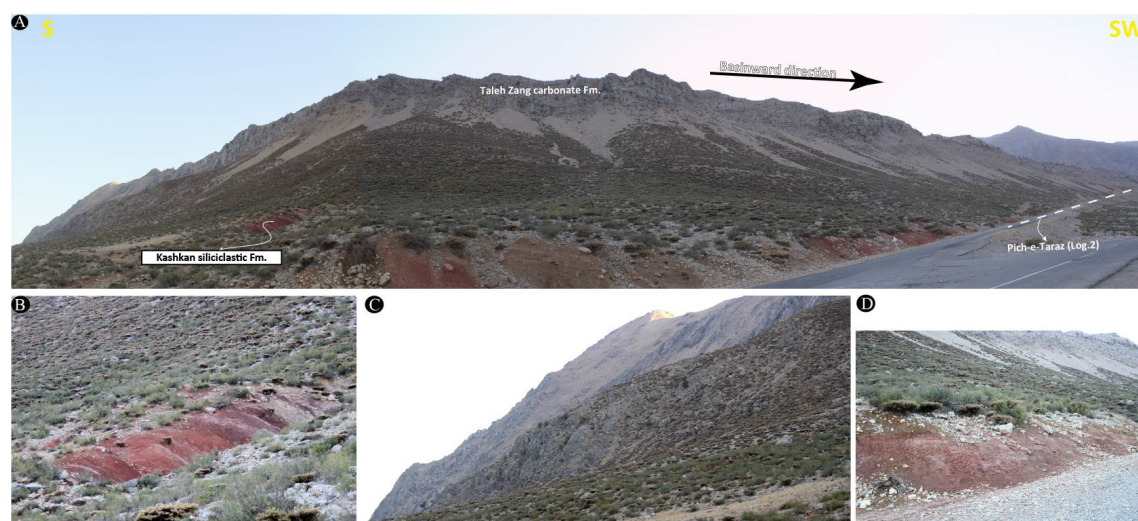


Figure 8. Overview outcrop (A) photographs of the northern flanks of the Keynow anticlines. It remarks Taleh Zang carbonate platforms covered by continental deposits of the Kashkan red-colored Formation (B and D). Note the location of log. 2 (Pich-e-Taraz) and basinward direction. C) Close up view of Fig. 9a

Age determination:

Age determination of the sediments is required for an acceptable sedimentary basin analysis, which may be accomplished using several age dating techniques such as biostratigraphy. As a result, the extensive presence of benthic and planktonic foraminifera in the examined region offered an ideal environment for conducting biozonation schemes, which resulted in the relative age dating of the sediments. Therefore, key identified-LBFs were categorized and dated in terms of the local biozonation scheme introduced by (Wynd 1965), whereas the age determination of planktonic foraminifera was based on the global biozonation presented by (Berggren & Pearson 2005).

In the Taraz section, key large benthic foraminifera are enriched in carbonate beds of the Tarbur and Taleh Zang formations, while interbedded argillaceous limestone beds and thin-bedded shales are represented by a diverse assemblage of planktonic foraminifera (fig. 10). In the Pich-e-Taraz section, basin-floor sediments only contain a variety of planktonic foraminifera (Figs. 6, and 13).

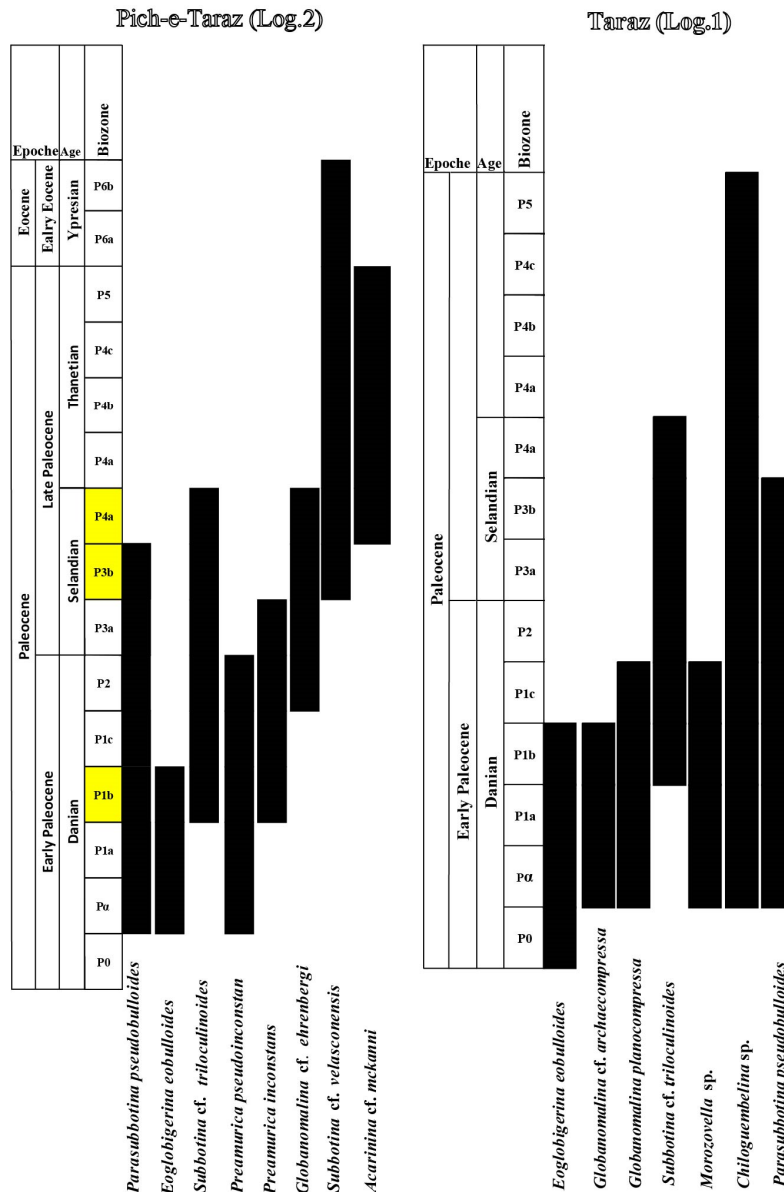


Figure 9. Biostratigraphical age dating of Taraz and Pich-e-Taraz sections based on planktonic foraminifera Zonation of Berggren and Pearson (2005)

In the Taraz section, the lowermost carbonate interval is dominated by rudist-debris fragments, which have been dated as Maastrichtian in age. The presence of abundant large benthic foraminifera (LBF), including *Orbitoides* sp. SCHWAGER, 1876, *Siderolites* sp. LAMARCK, 1801, and *Omphalocyclus macroporus* Lamarck, 1816, along with rudist debris, further confirms the Late Cretaceous age (Maastrichtian) (Wynd, 1965; Payandeh et al., 2019). Additionally, notable macroflora observed in the Tarbur Formation includes the dasycladaceae group, particularly accumulated in a portion of the Late Maastrichtian. These photosynthetic algae serve as an indicator of the photic zone, as their maximum effective depth of light penetration in water is 200 meters (Afghah, M., 2010) (Fig. 6 and 15).

Upsection towards younger successions, Cenozoic benthic foraminifera appeared. As such, some index fauna such as *Kathina* sp. and *Miscellanea yvettae* LEPPIG, 1988, 1983 and *Miscellanites Minutus* Rahaghi, 1983 with missing dominate presence of *Nummulites* sp. and *Alveolina* sp. are consistent with the Paleocene age. (Fig. 6 and 15).

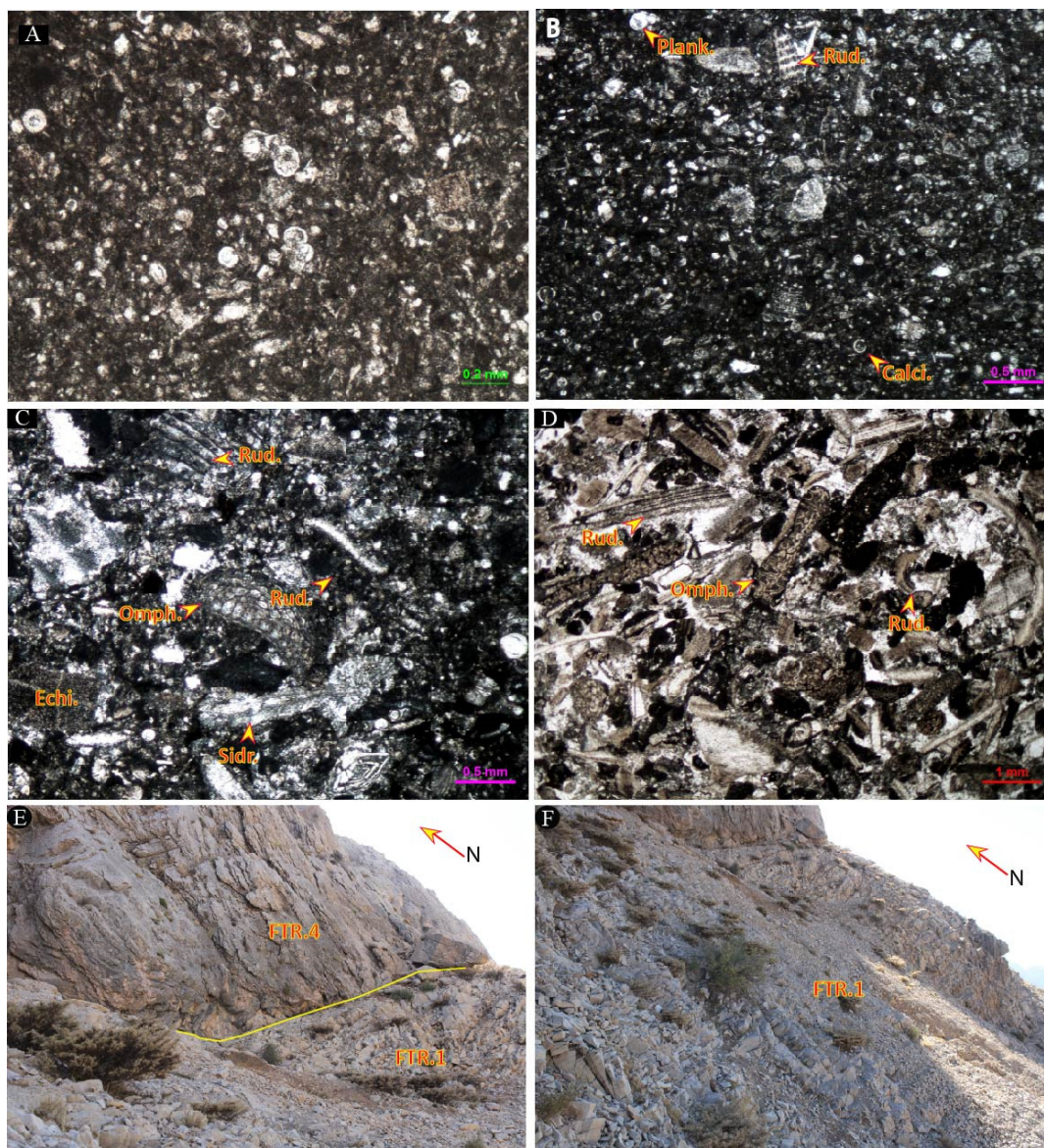


Figure 10. Photomicrographs and outcrop photograph of the Maastrichtian Tarbur facies (FTR). A; FTR.1: Planktonic foraminifera wackestone/packstone, B; FTR.2 (Planktonic fragmented-large benthic foraminifera wackestone/packstone), C; FTR.3 (Bioclast flattened large benthic foraminifera peloidal grainstone/packstone), D; FTR.4 (Bioclast Omphalocyclus peloidal Rudist deb. grainstone). Plank. Planktonic foraminifera, Rud. Rudist, Calci.: calcisphere, Echi.: Echinoid, Omph.: Omphalocyclus, Sidr.: Siderolites, E; mm-to cm-scale deep-water shale to marly limestone of FTR.1 and thick bedded of FTR.4 F; mm-to cm-scale deep-water shale to marly limestone of FTR.1

Among the planktonic foraminifera (Fig.10), *Eoglobigerina eobulloides*, *Globanomalina* cf. *archaeocompressa*, *Globanomalina planocompressa*, *Subbotina* cf. *triloculinoides*, *Globanomalina planocompressa*, *Morozovella* sp., and *Subbotina* cf. *triloculinoides*, correspond to Zone-P1b of (Berggren & Pearson, 2005), representing Lower Paleocene (Danian) (Fig. 9, and 11).

Other presence of taxa-i.e., *Morozovella conicotruncana*, *Igorina* cf. *albearti*, *Igorina* cf. *alberti*, *Chiloguembelina* sp., *Parasubbotina pseudobulloides*, *Parasubbotina pseudobulloides*, *Parasubbotina pseudobulloides*, *Subbotina* cf. *triloculinoides*, corresponds to Zone-P3b of Berggren and Pearson; 2005, confining to the late Paleocene (Selandian) (Figs. 9, 10 and 12).

The Pich-e-Taraz section, in contrast to the Taraz outcrop, lacks benthic foraminifera; however, there are abundant and varied presences of planktonic foraminifera (Figs. 9 and 13). As such, age determination of the sediments in this section was carried out based on the occurrence and distribution of planktonic fauna (Fig 13).

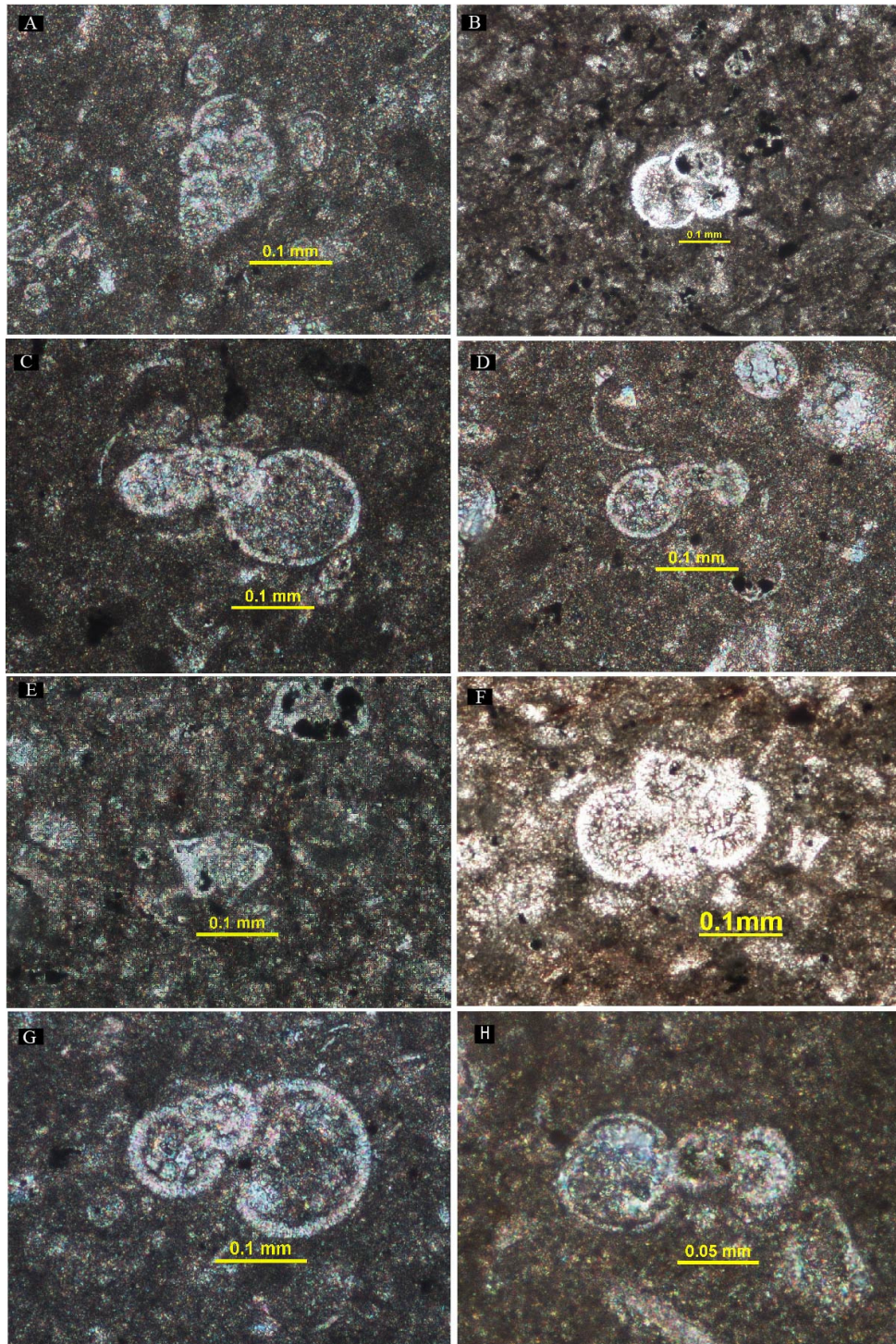


Figure 11. A: *Chiloguembelina* sp., B: *Eoglobigerina eobulloides*, C and H: *Globanomalina* cf. *Archaecompressa*, D: *Globanomalina planocompressa*, E: *Morozovella* sp., F: *Acarinina* cf. *mckanni*, G: *Subbotina* cf. *triloculinoides*, (corresponds to Zone-P1b of Berggren and Pearson (2005), representing Lower Paleocene (Danian))

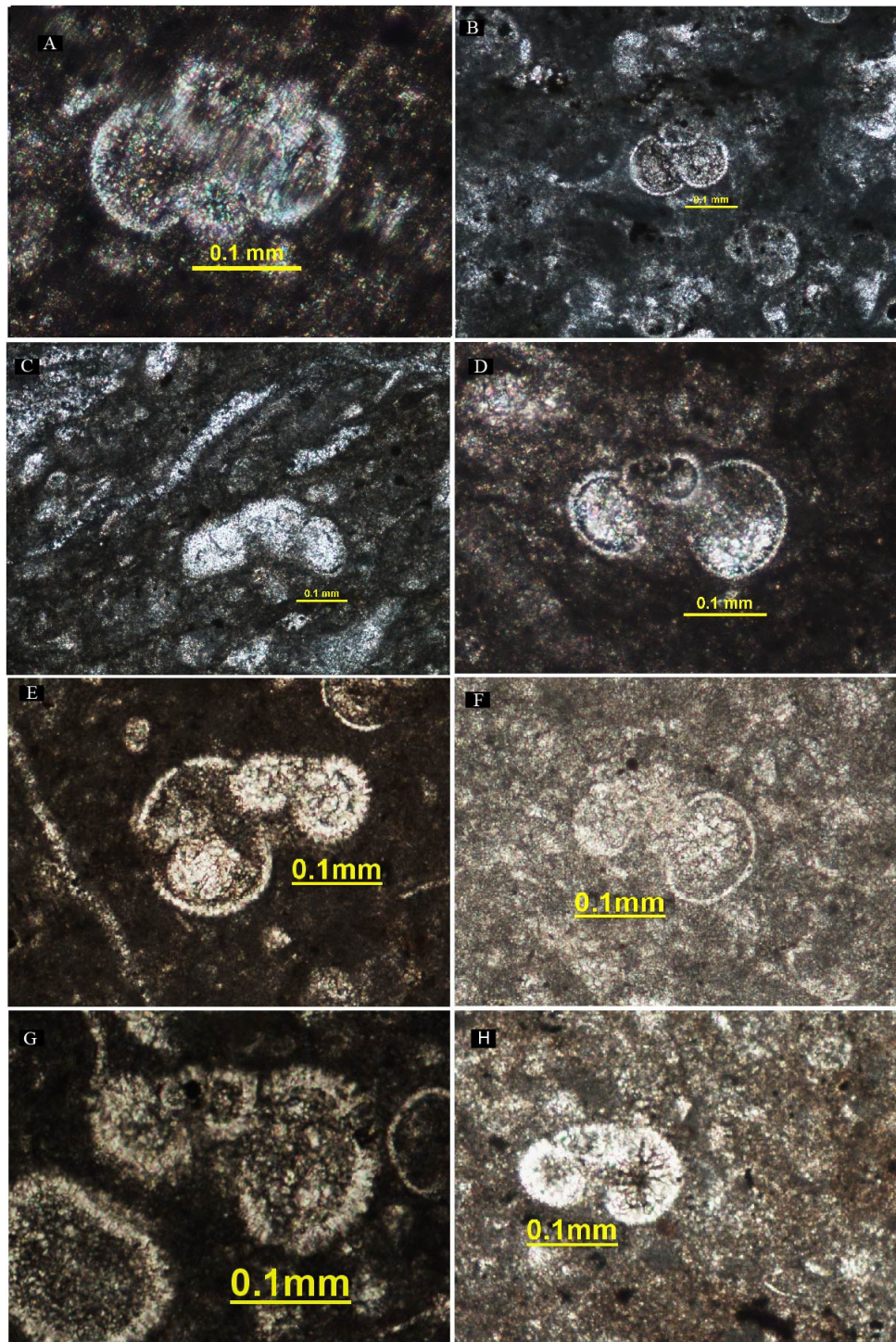


Figure 12. A: *Acarinina* cf. *mckanni*, B: *Eoglobigerina eobulloides*, C: *Globanomalina* cf. *ehrenbergi*, D: *Parasubbotina* cf. *pseudobulloides*, E: *Parasubbotina pseudobulloides* F: *Preamurica inconstans*, G: *Subbotina* cf. *triloculinoides* H: *Subbotina* cf. *velasconensis*, (corresponds to Zone-P3b of Berggren and Pearson (2005), assigning to late Paleocene (Selandian))

The partial appearance of *Parasubbotina pseudobulloides*, *Eoglobigerina eobulloides*, *Subbotina* cf. *triloculinoides*, *Preamurica pseudoinconstans*, *Preamurica inconstans*, *Subbotina* cf. *triloculinoides*, *Parasubbotina* cf. *pseudobulloides*, correspond to Zone-P1b of (Berggren & Pearson, 2005), assigning to early Paleocene (Danian) in age (Fig. 9).

Towards the uppermost successions, dominated presence of *Globanomalina* cf. *ehrenbergi*, *Subbotina* cf. *velasconensis*, and *Acarinina* cf. *mckanni* corresponds to Zone-P3b of (Berggren & Pearson, 2005), assigning to late Paleocene (Selandian) (Figs. 9, 12 and 13).

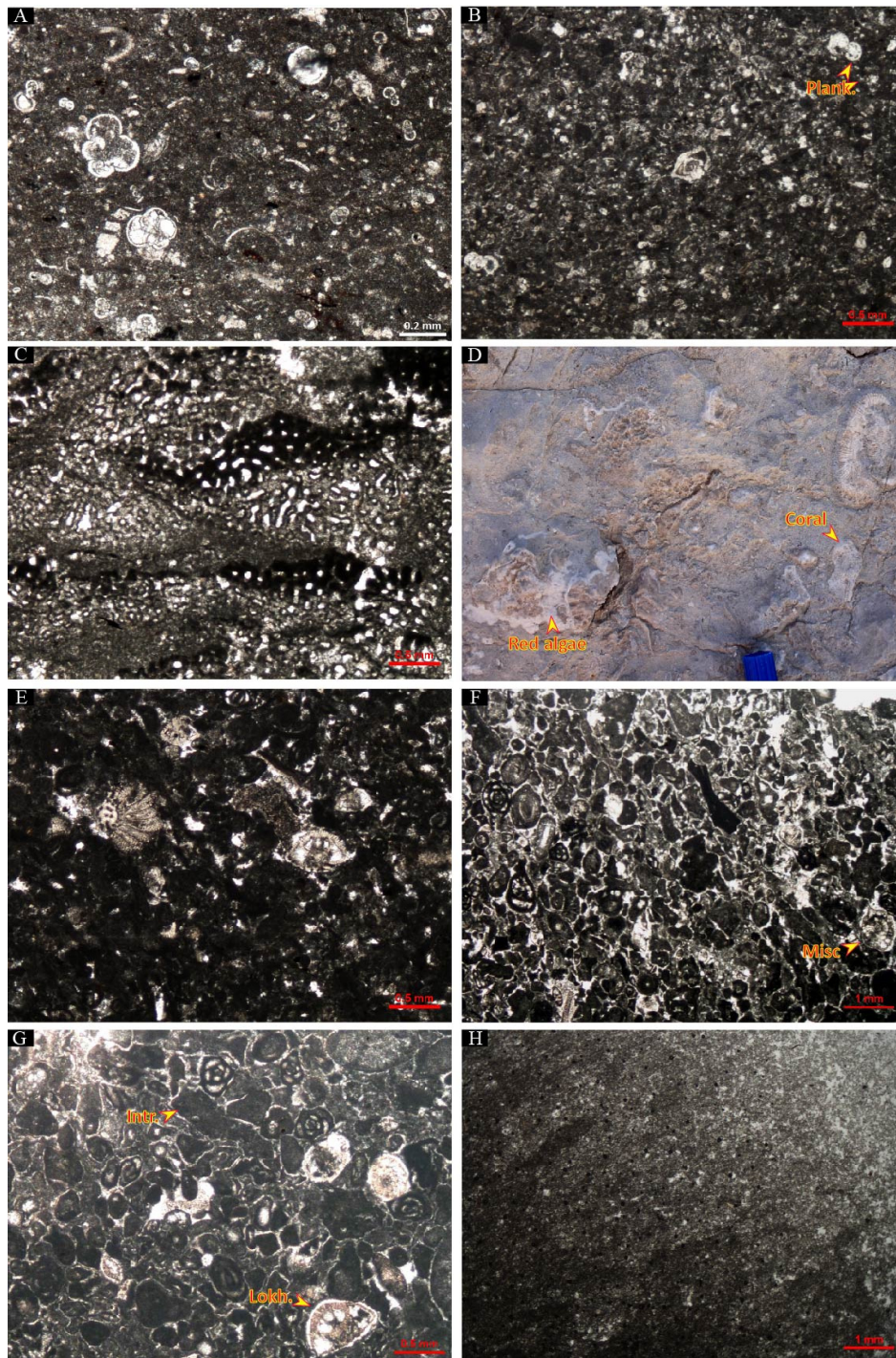


Figure 13. Photomicrographs and field photographs of the Paleocene Taleh Zang facies (FTZ). A; FTZ.1 (Bioclast Planktonic foraminifera wackestone/packstone), B; FTZ.2 (Bioclast Planktonic hyaline benthic foraminifera wackestone/ packstone), C and D; FTZ.3 (Bioclast coral coralline red algae boundstone), E; FTZ.4: (Bioclast *Miscellanea* miliolid peloid packstone-grainstone), F and G; FTZ.5 (Bioclast peloid miliolid grainstone/packstone), H; FTZ.6 (Dolo-mudstone). Plank. Planktonic foraminifera, Misc.: *Miscellanea*, Intr.: intraclast, Lokh.: *Lokhartia*

Facies Architecture and Depositional Environment

To gain a deeper understanding of depositional settings throughout the conceptual model, extensive macroscopic and microscopic investigations (sedimentary characteristics, fabric, skeletal, and non-skeletal grain relationships), as well as the apparent geometry of depositional successions, were carried out. Facies analysis is categorized based on (Dunham 1962; Embry and Klovan, 1971), and (Flügel, 2010). Furthermore, depositional interpretation of comparable facies in coeval or identical carbonate platforms was used throughout the Tethyan Basin. Consequently, 10 depositional facies were identified (Fig. 6); which are defined by two abbreviation names (FTR and FTZ), as described below. The FTR is related to the Tarbur carbonate Formation during the Maastrichtian, whereas the Taleh Zang Paleocene Formation is marked by the FTZ.

FTR.1: Planktonic foraminifera wackestone/packstone

This facies is composed of mm-to cm-scale deep-water shale to marly limestone with well-preserved planktonic foraminifera and calcispheres, with high diversity and abundance within a micrite matrix (Figs. 6 and 10 A). Fine-grained debris of echinoid and benthic foraminifera fragments transported from the shallower setting are additional bioclast elements (Fig. 10 A, E and F).

Both skeletal and fabric properties of facies suggest a deep-water basin in an aphotic zone (Flügel, 2010; Ghabeishavi et al., 2009; Pomar, 2001b; Pomar, 2020) belonging to the Amiran/Gurpi formations during the Maastrichtian (Fig. 6). Basinward, to the northwest, and west/southwest, this facies consists of an alternation of distal pelagic marl/shale and slightly sand/siltstone, representing the Amiran turbidity Formation that completely changes more basinward into planktonic-rich shales and argillaceous thin-bedded limestone, belonging to the basinal Gurpi Formation (Fig. 6).

FTR.2: Planktonic fragmented-large benthic foraminifera wackestone/ packstone

FTR.2 corresponds to the dm - to mt-scale limestone to argillaceous limestone beds (Fig. 6). A wackestone-packstone texture rich in fine-to-rare medium-grained bioclasts, typically accompanied by planktonic foraminifera and calcispheres, is the visible specification of this facies (Fig. 10 B). Major bioclast associations are evidenced by highly abraded hyaline benthic foraminifera, such as *Siderolites*, *Orbitoides*, *Omphalocyclus*, and undefined foraminifera, together with rare rudist and echinoid debris mostly sprayed within a micrite matrix (Fig. 10 B).

This facies shares the same carbonate-producing grains and textural properties as FTR.1, with the exception of a higher frequency of fine-to-medium-grained biota fragments, indicating a much shallower setting than the previous microfacies, presumably corresponding to the distal slope to toe slope settings of a carbonate platform (Janson et al., 2010; Pomar et al., 2012). (Fig. 6).

FTR.3: Bioclast flattened large benthic foraminifera peloidal grainstone/packstone

This facies consists of mt- to dm-scale limestone beds (Fig. 6). It is characterized by a grain-supported fabric with a grainstone-packstone texture (Fig. 10 C). The main components of this facies were poorly rounded benthic foraminifera and peloids. Hyaline large benthic foraminifera (e.g., *Omphalocyclus* and *Orbitoides*), *Loftusia*, small miliolids, and peloids are fundamental associations (Fig. 10 C). Rudist debris and particles of undefined benthic foraminifera, along with rare planktonic foraminifera, are minor constituents (Fig. 10 C).

Flattened LBF-i.e., *Omphalocyclus*, and *Orbitoides* along with poorly-rounded, fine-to-

medium grains and rudist fragments, mostly shed from shallower parts suggest that this facies was formed in the slope environment (Piryaei et al., 2010) under low to medium-energy (Ghabeishavi et al., 2010) (Fig. 6).

FTR.4: Bioclast Omphalocyclus peloidal Rudist deb. grainstone

FTR.4 is made up of mt-scale to enormous limestone strata that create cliffs (Fig. 6). A grainstone groundmass consists of a grain-supported matrix created by a well-sorted association of coarse-grained rudist debris, poorly preserved *Omphalocyclus*, poorly rounded skeletal components, and peloids (Fig. 10 D, E). Typically, there is no lime-mud matrix (Fig. 10 D). The additional components are mostly represented by small miliolids. FTR.4 laterally interfingered down-dip with FTR.3, in which both the frequency and size of rudist debris were significantly reduced (Fig. 6).

Textural, skeletal, and non-skeletal features lead this facies to deposit under a high-energy situation, which can be assigned to a shoal setting (Ghabeishavi et al., 2010) of a platform margin (Piryaei et al., 2010; Vincent et al., 2015), based on the ideal facies belts suggested by (Wilson, 1975) and (Flügel, 2010) (Fig. 6). It seems that FTR.4 changes landward to the NE into a grain-supported rudist-rich facies with buildup geometries (Fig. 6).

FTZ.1: Bioclast Planktonic foraminifera wackestone/packstone

This facies is evidenced by mm-to cm-scale shale to marly limestone rich in planktonic and slightly fine-grained, poorly-preserved benthic foraminifera fragments (Figs. 6, and 13A). *Miscellanea*, *Kathina*, and other undefined benthic foraminifera as *ex situ* components, along with rare echinoid debris were shed from shallower domains into the basinal wackestone-to-slightly packstone setting.

Massive amounts of hemipelagic and pelagic sediments of this facies, similar to the of FTR.1 during the Maastrichtian, represent a distal slope to the deep-water basin, in an aphotic zone (Allahkarampour Dill et al., 2018; Morsilli et al., 2012; Pomar, 2001a, 2001b, 2020; Pomar et al., 2012, 2014; Scheibner et al., 2003), belonging to the Amiran/Pabdeh formations during the Paleocene (Fig. 6).

FTZ.2.: Bioclast Planktonic hyaline benthic foraminifera wackestone/packstone

FTZ.2 is characterized by mt-to dm scale wackestone to wackestone-packstone rich in planktonic foraminifera and fine-to- medium grains of biogenic fragments presumably shed from shallower parts (Fig. 13 B) and (Fig 14 D). The lime-mud matrix contains fragments of undefined and well-defined benthic foraminifera, echinoids, unusual microscopic miliolids, coral, and coralline red algae (Fig.13 B). *Miscellanea* and *Kathina* pieces were found in greater numbers in the LBF than in the FTZ.1, but with lower species diversity, the frequency rate of planktonic foraminifera was lower. Under certain circumstances, Coral and red algae pieces may be found as secondary biota. A mixture of planktonic and re-sedimented benthic foraminifera associations indicates a distal-slope to toe slope setting of a carbonate ramp (Allahkarampour Dill et al., 2018; Pomar et al., 2012; Scheibner et al., 2003), reflecting an oligophotic to slightly dysphotic zone (Morsilli et al., 2012; Pomar, 2001b, 2020; Pomar et al., 2017, 2014) (Fig. 6).

FTZ.3: Bioclast coral coralline red algae boundstone

FTZ.3 is composed of mt- to dm-scale limestone beds (Fig. 6). It showed a boundstone texture

rich in discrete coral patches and coralline red algae fragments (Fig. 13 C, D). Benthic foraminifera and peloids are skeletal and non-skeletal elements that are rarely spread in this facies. FTZ.3 predominantly took place at the uppermost part of the Taleh Zang carbonate Formation in Log.1 (Fig. 6).

A rudestone floatstone texture is described as a cluster fabric with no major skeletal structure by discrete proportions of coarse- to medium-grained skeletal components inside a significant amount of micrite matrix (Pomar, 2020; Pomar et al., 2017; Riding, 2002). (Fig. 13). Therefore, the FTZ.3 shows the platform margin to upper-slope (middle ramp) settings, below bioclastic shoals of a carbonate ramp profile, built in a meso-oligophotic condition (Martín-Martín et al., 2020; Morsilli et al., 2012; Pomar, 2001a, 2001b, 2020; Pomar et al., 2017, 2014) (Fig. 6).

*FTZ.4: Bioclast *Miscellanea miliolid peloid* packstone-grainstone*

This facies is represented by mt- to dm- scale limestone beds (Fig. 6). It shows a well-rounded, well-sorted taxa-dominated packstone to grainstone (Fig. 13 E). Mostly Fine- to slightly medium-grained benthic foraminifera fragments, such as hyaline perforate types (e.g., *Miscellanea* and *Kathina*), along with well-rounded red algae, small miliolids, and peloids are outstanding elements of this facies dispersed in the grainstone-packstone matrix (Fig. 13 E). Well-rounded debris of coral, green algae and undefined benthic foraminifera together with shell fragments are additional components of the FTZ.4.

The presence of these skeletal and non-skeletal components, particularly highly abraded and mixed coarse grains, within a grainstone- to- packstone matrix suggests a high to medium energy shoal environment (Pomar, 2001b; Sarkar, 2015), accumulated in the wave-agitated, distal inner to the proximal middle ramp, laterally in a transition between restricted inner and slope settings (Fig. 6).

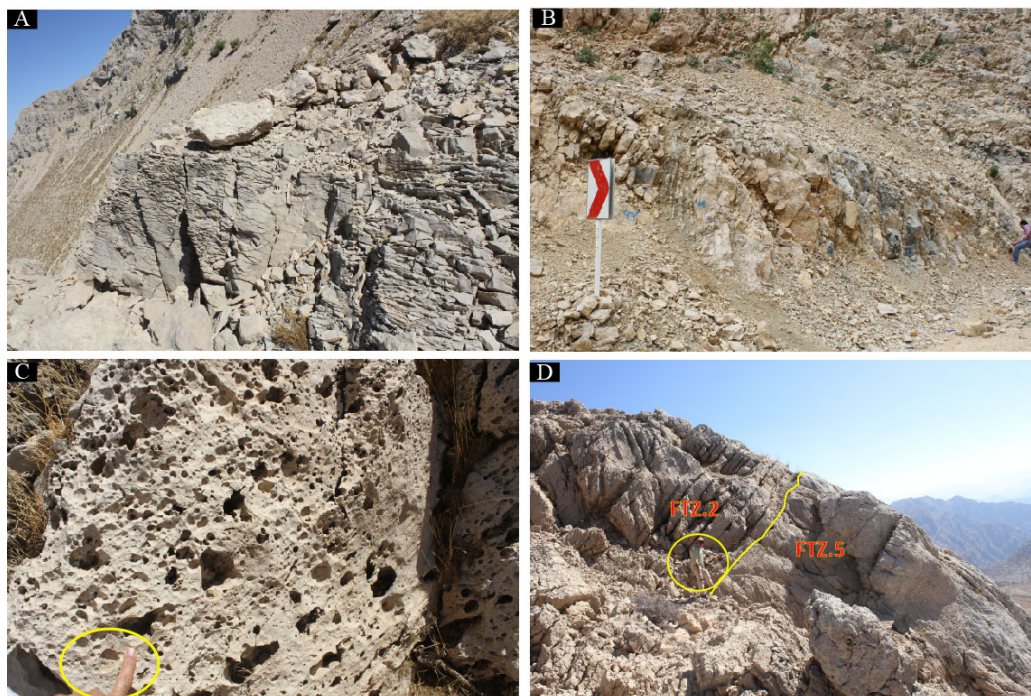


Figure 14. photographs of the Paleocene Taleh Zang facies (FTZ). A; mm-to cm-scale shale to marly limestone of FTZ.1. B; mm-to cm-scale shale to marly limestone rich in planktonic of FTZ.1. C; Karstification at the top of dolomitic facies of FTZ.6. D; mt-to dm scale wackestone to wackestone-packstone of FTZ.1 and mt- to dm scale grainstone- to packstone beds of FTZ.5. The marked circle refers to the person for scale

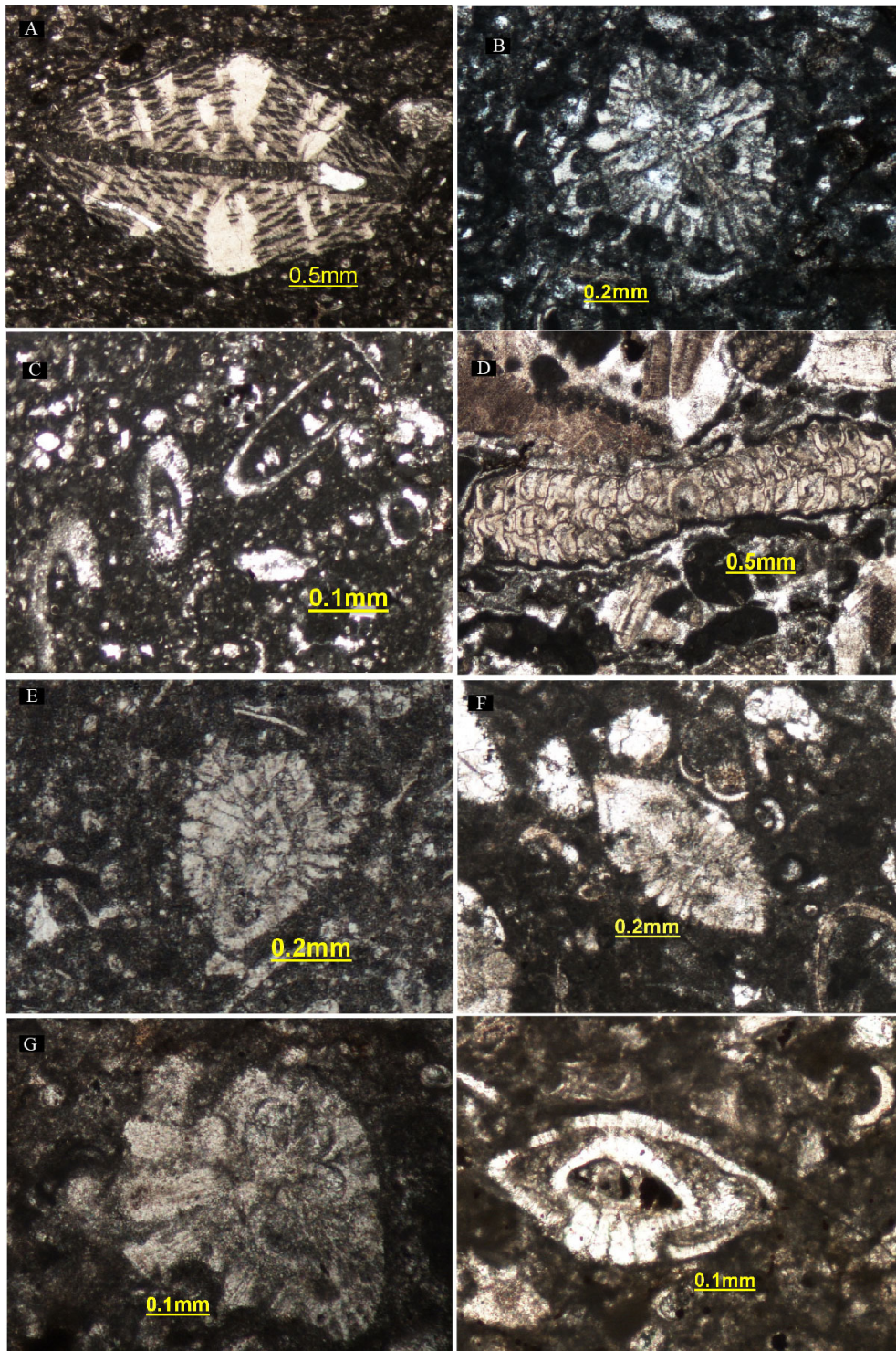


Figure 15. A: *Orbitoides* sp. (SCHWAGER, 1876), B: *Siderolites* sp. (LAMARCK, 1801), C: Dasycladaceae D: *Omphalocyclus macroporus* (Lamarck, 1816) E: *Miscellanea yvetteae* (LEPPIG, 1988) F: *Miscellanites minutus* (RAHAGHI, 1983), G: *Lockhartia Conditi* Nutgall, 1926, H: *Kathina Delseota* Smout, 1954

FTZ.5: Bioclast peloid miliolid grainstone/packstone

This facies is built of mt- to dm- scale grainstone- to slightly packstone beds (Fig. 13F, G) and

(Fig 14 D). Both well-rounded and well-sorted components, such as small miliolids, peloids, and rarely ex situ green algae within a high-energy grainstone matrix are the most important elements of this facies (Fig. 13 F, G); however, *Miscellanea* and *kathina*, with lesser amounts present. Secondary bioclast pieces include Textularids, Red algae, echinoid fragments, and undefined benthic foraminifera. Green algae, ooids, and intraclast pieces (Fig. 13 G) were also visible in certain thin slices. Occasionally, *Miscellanea*, *Kathina*, and *Miliolids* serve as the nuclei of ooids. Numerous abraded and rounded lagoonal grains of porcelaneous benthic foraminifera together with well-rounded taxa, for example, peloid, sand, and ooids within a grainstone matrix suggest a leeward side of a shoal environment (Bagherpour & Vaziri, 2012), placed in the euphotic, inner ramp (Bassi & Nebelsick, 2010; Martín-Martín et al., 2020) (Fig. 6); in which hyaline foraminifera types are rare. This facies grade landward into more restricted environments (FTZ.6) (Fig. 6).

FTZ.6: Dolo-mudstone

This facies is marked by dm-scale dolomite to dolo-mudstone (Fig. 6). The texture is mostly composed of fine- to coarse dolomite to dolo-micrite crystals with no fossil content (Figs. 6, and 13 H). In some cases, a mudstone texture with a ghost to rare fossil elements, for example planktonic foraminifera is present. This facies is embedded in deep-water facies (FTZ. 1 and 2). Petrographical (ghost of planktonic foraminifera) and the stratigraphical position suggest that this facies is secondary diagenetic dolomite (e.g., Gregg 1985; Lee & Friedman, 1987; Amthor & Friedman, 1991). Karstification at the top of this dolomitic facies (Figs. 6, and 14 C) as a significant bounding surface most likely caused the dolomitization process.

Discussion

Depositional models

These facies are categorized from the distal to proximal areas of the depositional basin based on the spatial and temporal distribution of grain associations and other depositional and biological characteristics. From the Maastrichtian to the Paleocene, two distinct depositional models, namely the Tarbur carbonate ramp (FTR) and the Taleh Zang carbonate ramp (FTZ), emerged. 6.2. Maastrichtian distally steepened Tarbur carbonate ramp:

Tarbur carbonate ramp, Maastrichtian in age, is composed of thick-bedded limestone deposits of the Tarbur Formation in log-1. (Taraz Section). It consists of four facies, namely FTR.1, FTR.2, FTR.3, and FTR.4, which are rich in rudist communities, and LBF, which shortly towards NWW grades entirely into basinal deep-water deposits of the Amiran/Gurpi Formation (log-2; Pich-e-Taraz section). Therefore, this platform shows a lateral distribution of the middle to outer segments of a NE-NWW stretched distally steepened ramp profile (Fig. 6). More restricted environments are deposited most likely towards the NE, which are located outside of this study.

Paleocene Taleh Zang carbonate ramp:

After K/Pg. boundary, massive flooding of the Paleocene sea, which is represented by thick-bedded, deep-water shales of the Amiran/Pabdeh Formation, abruptly transgressed onto the former carbonate platform so that it could fully drown the Tarbur carbonate ramp. Following the subsequent sea-level stand, carbonate platform deposits of the Taleh Zang Paleocene Formation accumulated. From the proximal carbonate platform to the basin, the Taleh Zang carbonate ramp consists of six sedimentary facies (FTZ.1- 6) (Fig. 6). The description,

interpretation, and lateral distribution of these identified facies supported by field observations reveal proximal-inner, middle, and outer to the deep-water basin of a carbonate ramp elongated, inconsistent with the preceding carbonate platform but with a lower steep angle, from the NE (Log. 1) to NW-W (log). 2) (Fig. 6). In fact, the proximal-inner-to-middle settings of the carbonate ramp are positioned towards the NE (Log. 1; Taraz). In contrast, the carbonate Taleh Zang ramp gradually pinched out into the outer ramp to deep-water basin deposits to NW-W; in which the Amiran/Pabdeh Formation including thin-bedded limestone and shales rich in planktonic foraminifera are accumulated in Log. 2 (Pich-e-Taraz).

From the upper Selandian onwards, the first dominated community of Cenozoic Zooxanthellate corals started to thrive in the study area after K/Pg. boundary (Martín-Martinet et al., 2021) (Fig. 6). Based on the first presence of these coral colonies, the Taleh Zang carbonate ramp was differentiated into two distinct carbonate modes: a Danian-lower Selandian carbonate ramp with no coral colonies and an upper Selandian coral-bearing carbonate ramp (Fig. 6). As such, the Danian-lower Selandian carbonate ramp is the first carbonate platform accumulated at the start of the Cenozoic, containing mostly a low diversity of medium-to fine-grained benthic foraminifera, that is, *Miscellanea* and *Kathina*, together with well-rounded miliolids and peloids with no coral fragments (Fig. 6). This carbonate platform was older than the time interval evaluated by (Scheibner & Speijer 2008a, 9).

The habitat and climatic conditions in the upper Selandian offered an ideal setting for growing initial coral colonies, with discrete coral patches occupying the mesophotic zone of the marginal middle ramp environment (Fig. 6). Consequently, the upper Selandian carbonate platform is similar to (Scheibner & Speijer's, 2008a, 2008b) platform stage II, which is characterized by the coexistence of coral fragments and LBF.

Conclusion:

In this paper, a platform-to-basin transition at the NE Arabian passive margin in the proximity of the hinterland and obducted ophiolite complex was studied. It contains two well-exposed sections: Taraz (log-1) and Pich-e-Taraz (Log-2); placed at the proximal and distal domains. Based on the emergence and extinction events of significant LBF completed by planktonic foraminifera prevalent in interlayered shales, these carbonate layers are dated to the Maastrichtian (Tarbur Formation) and lower Paleocene (Danian-Selandian; Taleh Zang Formation). Ten sedimentary facies for the Tarbur Formation (FTR) and Taleh Zang (FTZ) were determined based on biological evolution and facies analyses. From proximal to distal, FTR.4 to FTR.1 remark middle, outer to deep-water basin settings of a distally steepened ramp during Maastrichtian (Tarbur Formation). By lower Paleocene (Danian- Selandian), in contrast, following basin evolution and appearance of different evolved biota after the K/T boundary, FTZ.6, 5, 4, 2, and 1 show inner, middle, outer to the deep-water basin of a carbonate ramp elongated, inconsistency with preceding carbonate platform (Tarbur) but with a minor steep angle, from the NE to the SW. As a consequence of thriving first Z-corals together with coralline red algae (FTZ.3); the lower Paleocene carbonate platform was separated into two distinct carbonate modes: a Danian-lower Selandian carbonate ramp with no coral colonies and an upper Selandian coral-bearing carbonate ramp. The first carbonate ramp (Danian-lower Selandian) is older than the time interval evaluated by (Scheibner & Speijer, 2008a, 2008b); although the second one is attributed to platform stage II of (Scheibner & Speijer 2008a, 2008b).

References

- Afghah, M. 2010. Biozonation and biostratigraphic limits of the Tarbur Formation around Shiraz (SW of Iran). PhD Thesis University of Münster, 49.
- Alavi, M., 1994, Tectonics of the Zagros orogenic belt of Iran: new data and interpretations:

- Tectonophysics, 229: 211-238.
- Alavi, M., 2004, Regional stratigraphy of the Zagros fold-thrust belt of Iran and its proforeland evolution: *American Journal of Science*, 304: 1-20.
- Allahkarampour Dill, M., Vaziri-Moghaddam, H., Seyrafian, A., and Behdad, A., 2018, Oligo-Miocene carbonate platform evolution in the northern margin of the Asmari intra-shelf basin, SW Iran: *Marine and Petroleum Geology*, 92: 437-461.
- Amiri-Bakhtiyar, H., Shemirani, A., Sadeghi, A., Adabi, M. H., and Vaziri-Moghaddam, H., 2006, Reappraisal of boundary between the Tarbur and Sachun Formations in Fars area (Zagros- Iran): *Journal of Earth Science*, Shahid Beheshti University, Tehran, 16: 3-9. (In persian with english abstract).
- Amthor, J. E., and Friedman, G. M., 1991, Dolomite-rock textures and secondary porosity development in Ellenburger Group carbonates (Lower Ordovician), west Texas and southeastern New Mexico: *Sedimentology*, 38: 343-362.
- Baceta, J. I., Pujalte, V., and Bernaola, G., 2005, Paleocene corallgal reefs of the western Pyrenean basin, northern Spain: New evidence supporting an earliest Paleogene recovery of reefal ecosystems: *Palaeogeography, Palaeoclimatology, Palaeoecology*, 224 : 117- 143.
- Bagherpour, B., and Vaziri, M. R., 2012, Facies, paleoenvironment, carbonate platform and facies changes across Paleocene Eocene of the Taleh Zang Formation in the Zagros Basin, SW-Iran: *Historical Biology*, 24, : p. 121-142.
- Bassi, D., and Nebelsick, J. H., 2010, Components, facies and ramps: Redefining Upper Oligocene shallow-water carbonates using coralline red algae and larger foraminifera (Venetian area, northeast Italy): *Palaeogeography, Palaeoclimatology, Palaeoecology*, 295: 258-280.
- Berberian, M., and King, G. C. P., 1981, Towards the paleogeography and tectonic evolution of Iran: *Canadian Journal of Earth Sciences*, 18: 210-265.
- Berggren, W. A., and Pearson, P. N., 2005: A revised tropical to subtropical Paleogene planktonic foraminiferal zonation *Journal of Foraminiferal Research*, 35: 279-298.
- Dunham, R. J., 1962, Classification of carbonate rocks according to depositional texture, in Ham, W. E., ed., *Classification of Carbonate Rocks*, AAPG Mem, 1: 108-121.
- Embry, A., and Klovan, J., 1971, a late Devonian reef tract on northeastern Banks Island, NWT: *Bulletin of Canadian Petroleum Geology*, 19: 730.
- Farsi): *Geol. Surv. Of Iran*, Tehran, v. 1.
- Flügel, E., 2010, *Microfacies of Carbonate Rocks, Analysis, Interpretation and Application*, Berlin, Springer-Verlag, 976
- Ghabeishavi, A., Vaziri-Moghaddam, H., and Taheri, A., 2009, Facies distribution and sequence stratigraphy of the Coniacian–Santonian succession of the Bangestan Palaeo-high in the Bangestan Anticline, SW Iran: *Facies*, 55: 243-257.
- Ghabeishavi, A., Vaziri-Moghaddam, H., Taheri, A., and Taati, F., 2010, Microfacies and depositional environment of the Cenomanian of the Bangestan anticline, SW Iran: *Journal of Asian Earth Sciences*, 37: 275-285.
- Glennie, K. W., 2000, Cretaceous tectonic evolution of Arabia's eastern plate margin: A tale of two oceans, in Alsharhan, A. S., and Scott, R. W., eds., *Middle East models of Jurassic/Cretaceous carbonate systems*, Society of Economic Paleontologists and Mineralogists Special Publication, 69: 9-20.
- Golonka, J., 2004, Plate tectonic evolution of the southern margin of Eurasia in the Mesozoic and Cenozoic: *Tectonophysics*, 381: 235-273.
- Gregg J. M., 1985, Regional epigenetic dolomitization in the Bonnetterre Dolomite (Cambrian), southeastern Missouri: *Geology*, 13: 503-506.
- Homke, S., Vergés, J., Beek, P. v. d., Fernández, M., Saura, E., Barbero, L., Badics, B., and Labrin, E., 2009a, Insights in the exhumation history of the NW Zagros from bedrock and detrital apatite fission-track analysis: evidence for a long-lived orogeny: *Basin Research*, 22: 659–680.
- Homke, S., Vergés, J., Serra-Kiel, J., Bernaola, G., Sharp, I., Garcés, M., Montero-Verdú, I., Karpuz, R., and Goodarzi, M. H., 2009b, Late Cretaceous—Paleocene formation of the proto—Zagros foreland basin, Lurestan Province, SW Iran: *Geological Society of America Bulletin*.
- James, G. A., and Wynd, J. G., 1965, Stratigraphic nomenclature of Iranian Oil Consortium Agreement Area: *AAPG Bulletin*, 49: 2182-2245.

- Janson, X., Van Buchem, F. S. P., Dromart, G., Eichenseer, H. T., Dellamonica, X., Boichard, R., Bonnaffe, F., and Eberli, G., 2010, Architecture and facies differentiation within a Middle Miocene carbonate platform, Ermenek, Mut Basin, southern Turkey: Geological Society, London, Special Publications, 329.
- Lee Y. I., and Friedman, G. M., 1987, Deep-burial diagenitization in the Lower Ordovician Ellenburger Group carbonates in western Texas and southeastern New Mexico: *Jour. Sed. Petrology*, 57: 544-557.
- Martín-Martín, M., Guerrero, F., Tosquella, J., and Tramontana, M., 2020, Paleocene-Lower Eocene carbonate platforms of westernmost Tethys: *Sedimentary Geology*, 404: 105,674.
- Morsilli, M., Bosellini, F. R., Pomar, L., Hallock, P., Aurell, M., and Papazzoni, C. A., 2012, Mesophotic coral buildups in a prodelta setting (Late Eocene, southern Pyrenees, Spain): a mixed carbonate-siliciclastic system: *Sedimentology*, 59: 766-794.
- Motiei, H., 1994, Stratigraphy of Zagros (in Farsi): *Geol. Surv. Of Iran*.
- Motiei, H., 1995, Petroleum geology of Zagros (in Farsi): *Geol. Surv. of Iran*, Tehran, 1.
- Nikfard, M. (2023). Lower Eocene carbonate ramp clinoforms of the southern Tethys; Zagros Foreland Basin, SW Iran: Sequence stratigraphy architecture, basin physiography and carbonate factory controlling parameters. *Basin Research*, 00: 1–29.
- Payandeh S, Afghah M, Parvaneh Nejad Shirazi M (2018) Biostratigraphy and lithostratigraphy of Tarbur Formation (Upper Cretaceous) in Hossein Abad section, Zagros basin (SW of Iran). *Carbonates Evaporites* 34:931–939
- Piryaei, A., Reijmer, J. J. G., van Buchem, F. S. P., Yazdi-Moghadam, M., Sadouni, J., and Danelian, T., 2010, The influence of Late Cretaceous tectonic processes on sedimentation patterns along the northeastern Arabian plate margin (Fars Province, SW Iran): Geological Society, London, Special Publications, 330: 211-251.
- Pomar, L., 2001a, Ecological control of sedimentary accommodation: evolution from a carbonate ramp to rimmed shelf, Upper Miocene, Balearic Islands: *Palaeogeography, Palaeoclimatology, Palaeoecology*, 175: 249-272.
- Pomar, L., 2001b, Types of carbonate platforms: a genetic approach: *Basin Research*, 13: 313-334.
- Pomar, L., 2020, Chapter 12 - Carbonate systems, in Scarselli, N., Adam, J., Chiarella, D., Roberts, D. G., and Bally, A. W., eds., *Regional Geology and Tectonics (Second Edition)*, Elsevier, p. 235-311.
- Pomar, L., and Haq, B. U., 2016, Decoding depositional sequences in carbonate systems: Concepts vs experience: *Global and Planetary Change*, 146: 190-225.
- Pomar, L., and Kendall, C. G. S. C., 2008, Architecture of carbonate platforms; a response to hydrodynamics and evolving ecology, in *Controls on Carbonate Platform and Reef Development*, J. Lukasik & A. Simo (Eds.): *SEPM Special Publication*, 89: 187-216.
- Pomar, L., Baceta, J. I., Hallock, P., Mateu-Vicens, G., and Basso, D., 2017, Reef building and carbonate production modes in the west-central Tethys during the Cenozoic: *Marine and Petroleum Geology*, 83: 261-304.
- Pomar, L., Bassant, P., Brandano, M., Ruchonnet, C., and Janson, X., 2012, Impact of carbonate producing biota on platform architecture: Insights from Miocene examples of the Mediterranean region: *Earth-Science Reviews*, 113: 186-211.
- Pomar, L., Mateu-Vicens, G., Morsilli, M., and Brandano, M., 2014, Carbonate ramp evolution during the Late Oligocene (Chattian), Salento Peninsula, southern Italy: *Palaeogeography, Palaeoclimatology, Palaeoecology*, 404: 109-132.
- Riding, R., 2002, Structure and composition of organic reefs and carbonate mud mounds: concepts and categories: *Earth-Science Reviews*, 58: 163-231.
- Sarkar, S., 2015, Thanetian–Ilerdian coralline algae and benthic foraminifera from northeast India: microfacies analysis and new insights into the Tethyan perspective: *Lethaia*, 48: 13-28.
- Saura, E., Verges, J., Homke, S., Blanc, E., Serra-Kiel, J., Bernaola, G., Casciello, E., Fernandez, N., Romaine, I., Casini, G., Embry, J. C., Sharp, I. R., and Hunt, D. W., 2011, Basin architecture and growth folding of the NW Zagros early foreland basin during the Late Cretaceous and early Tertiary: *Journal of the Geological Society*, 168: 235-250.
- Scheibner, C., and Speijer, R. P., 2009, Recalibration of the Tethyan shallow-benthic zonation across the Paleocene-Eocene boundary: the Egyptian record: *Geologica Acta*, 7: 195-214.
- Scheibner, C., and Speijer, R. P., 2008a, Decline of coral reefs during late Paleocene to early Eocene

- global warming: *eEarth*, 3: 19-26.
- Scheibner, C., and Speijer, R. P., 2008b, Late Paleocene-early Eocene Tethyan carbonate platform evolution -- A response to long- and short-term paleoclimatic change: *Earth-Science Reviews*, 90: 71-102.
- Scheibner, C., Rasser, M. W., and Mutti, M., 2007, The Campo section (Pyrenees, Spain) revisited: Implications for changing benthic carbonate assemblages across the Paleocene-Eocene boundary: *Palaeogeography Palaeoclimatology Palaeoecology*, 248: 145-168.
- Scheibner, C., Reijmer, J. J. G., Marzouk, A. M., Speijer, R. P., and Kuss, J., 2003, from platform to basin: the evolution of a Paleocene carbonate margin (Eastern Desert, Egypt): *International Journal of Earth Sciences*, 92: 624-640.
- Scheibner, C., Speijer, R. P., and Marzouk, A. M., 2005, Turnover of larger foraminifera during the Paleocene-Eocene Thermal Maximum and paleoclimatic control on the evolution of platform ecosystems: *Geology*, 33: 493.
- Sherkati, S., Letouzey, J., and Lamotte, D. F. d., 2006, Central Zagros fold-thrust belt (Iran): New insights from seismic data, field observation, and sandbox modelling: *TECTONICS*, 25: 1-27.
- Stöcklin, J., 1968, Structural history and tectonics of Iran. A review: *American Association of Petroleum Geologists Bulletin*, 52: 1229-1258.
- Stoneley, R., 1990, The Arabian continental margin in Iran during the Late Cretaceous: *Geological Society, London, Special Publications*, 49: 787-795.
- Vaziri-Moghaddam, H., Safari, A., and Taheri, A., 2005, Microfacies, paleoenvironments and sequence stratigraphy of the Tarbur Formation in Kherameh area, SW Iran: *Carbonates and Evaporites*, 20: 131-137.
- Vincent, B., van Buchem, F. S. P., Bulot, L. G., Jalali, M., Swennen, R., Hosseini, A. S., and Baghbani, D., 2015, Depositional sequences, diagenesis and structural control of the Albian to Turonian carbonate platform systems in coastal Fars (SW Iran): *Marine and Petroleum Geology*, 63: 46-67.
- Wilson, J. L., 1975, *Carbonate Facies in Geologic History*, New York, Springer-Verlag, 471
- Wynd, J. G., 1965, Biofacies of the Iranian consortium- agreement area: Iranian Offshore Oil Company.

